Path Following With a Fixed-Wing UAV

T. Espinoza-Fraire[1,*] and J.A. Sáenz[1]

[1]Facultad de Ingeniería, Ciencias y Arquitectura de la Universidad Juárez del Estado de Durango, Gómez Palacio, Durango, México

Abstract: This work presents four control laws applied to path following with a fixed-wing unmanned aerial vehicle, and such control laws are compared to know which of them achieved the control objective with a minor error and control effort. The control laws to compare are Proportional-derivative, Sliding Mode Control (SMC), Nested Saturations, and Fuzzy Logic. The results are obtained after several simulations using the Matlab-Simulink software.

Keywords: Path following, Control Laws, Fixed-Wing, Unmanned.

1. INTRODUCTION

The development and use of fixed-wing unmanned aerial systems (UAVs) are still increasing, but many areas still need to be developed, and one of them is the path following [1-2].

In the scientific literature, it is possible to find some research about this subject, as mentioned in [3] proposed a robust control to follow a trajectory based on virtual points with a fixed-wing UAV, and the results are presented in simulations.

In [4] a fixed-wing UAV with modeling based on three-dimensional, and path-following control. The strategy of control is that the outer-loop and the path-following control law developed relies on a nonlinear control strategy derived at the kinematic level, while the inner-loop consists of L1 adaptive augmentation loop is designed to meet strict performance requirements in the presence of unmanned aerial vehicle modeling uncertainty and environmental disturbances, and the results are presented in a real flight test.

Another form to resolve the path following UAVs is proposed in [5], and it focuses on correcting the error during the flight process of a UAV. Also, the Lyapunov theory is used in [6] to obtain a nonlinear control to follow a trajectory with fixed-wing UAVs.

Many times the fixed-wing UAV is very likely to deviate from the initial path generated by a path planning algorithm or desired trajectory, thus, in [7] is presented an algorithm to minimize the trajectories to achieve the desired trajectory in less time and avoid the deviation of the fixed-wing UAV.

In this work, we propose four control laws, one is linear (PD) and three nonlinear (Sliding Mode Control (SMC), Nested Saturations, and Fuzzy Logic). These controllers are compared in order to know the better performance to follow a predefined flight path with a fixed-wing UAV, and based on the error and control effort conclude the better controller for this mission.

The organization of this work is: Section II presents the equations to define altitude and lateral motion. The control law methodologies, it is presented in section III. Section IV presents the simulation results. Finally, in the section V are presented the conclusions.

2. FIXED-WING DYNAMICS

The aerodynamic model has been obtained based on Newton's second law of motion, some considerations are taken to obtain the model, that is, the earth is considered as a plane because the fixed-wing unmanned aerial vehicle will be traveling short distances in flight, and no flexible part of the aircraft is considered for the dynamic model. Then, the longitudinal model of the aircraft has been defined as [8]:

$$\dot{V} = \frac{1}{m}\left(-D + T\cos(\alpha) - mg\sin(\gamma)\right) \tag{1}$$

$$\dot{\theta} = q \tag{2}$$

$$\dot{q} = M_q q + M_{\delta_e}\delta_e \tag{3}$$

$$\dot{h} = V\sin(\theta) \tag{4}$$

where V is the relative flight speed, α describes the angle of attack, γ represents the angle of incidence of the wind and θ denotes the pitch angle. Also, *q* is the angular pitch velocity (concerning the y-axis on the body of the fixed-wing UAV). *T* denotes the engine thrust force, *h* is the altitude of the fixed-wing UAV and δ_e represents the deflection of the control surface, known in aerodynamics as lift [8-9], see Figure **1**. The aerodynamic effects on the UAV are obtained by the lift force *L* and the opposing force to the motion *D*. The

*Address correspondence to this author at the Faculty of Engineering, Science and Architecture, University Juarez of the Durango State, México;
E-mail: tadeo1519@gmail.com

E-ISSN: 2409-9694/24

total mass of the aircraft is given by *m*, *g* is the gravitational constant, I_{yy} describes the *y* component of the diagonal of the inertia matrix. The value of the angle of attack is obtained using the following relation. $\alpha = \theta - \gamma$ [10]. In aerodynamics, M_q and M_{δ_e} are the stability derivatives implicit in the pitching motion. The lift force L, and the force D are defined as [9]-[10]:

$$L = \bar{q} S C_L$$

$$D = \bar{q} S C_D$$

with $\bar{q}$ denotes the aerodynamic pressure. *S* is the wing area and $\bar{c}$ is the standard chord response. C_D and C_L are the aerodynamic coefficients for the lift and opposition forces, respectively [8]. The derivatives of aerodynamic stability are defined by:

$$M_q = \frac{\rho S V \bar{c}^2}{4 I_{yy}} C_{mq}$$

$$M_{\delta_e} = \frac{\rho V^2 S \bar{c}}{2 I_{yy}} C_{m_{\delta_e}}$$

where ρ is the air density (1.05 kg/m^3), S is the wing area (0.09 m^2), $\bar{c}$ is the standard chord response (0.14 m), b is the wingspan, I_{yy} defines the moment of inertia in pitch (0.17 kgm^2), C_{mq} Is the dimensionless coefficient for longitudinal motion, obtained experimentally (-50), $C_{m\delta e}$ defines the dimensionless coefficient for the elevator motion, obtained experimentally (0.25).

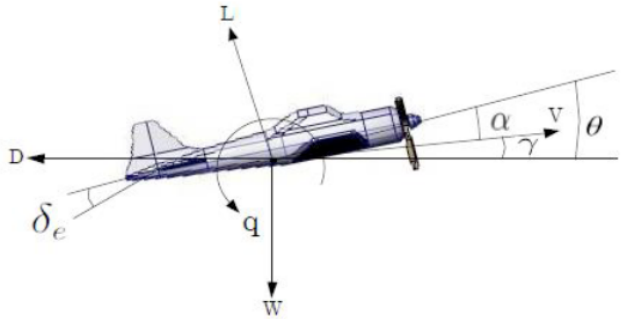

Figure 1: Pitch motion.

For yaw angle control the following aerodynamic model is considered:

$$\dot{\psi} = r \tag{5}$$

$$\dot{r} = N_r r + N_{\delta_r} \delta_r \tag{6}$$

where ψ defines the yaw angle, r Is the angular rate in the z-axis, δ_r defines the control surface called the stabilizer, see Figure **2**. N_r and $N_{\delta r}$ are the aerodynamic coefficients corresponding to the yaw angle control, and are defined by:

$$N_r = \frac{\rho S V b^2}{4 I_{zz}} C_{n_r}$$

$$N_{\delta_r} = \frac{\rho V^2 S b}{2 I_{zz}} C_{n_{\delta_r}}$$

with b as the size of the wingspan (0.914 m) of the fixed-wing unmanned aerial vehicle. Also, C_{nr} is the dimensionless coefficient for longitudinal motion, obtained experimentally (-0.01), $C_{n\delta r}$ defines the dimensionless coefficient for the elevator motion, obtained experimentally (0.0005). The inertial moment in the z-axis is defined by I_{zz} (0.02 kgm^2).

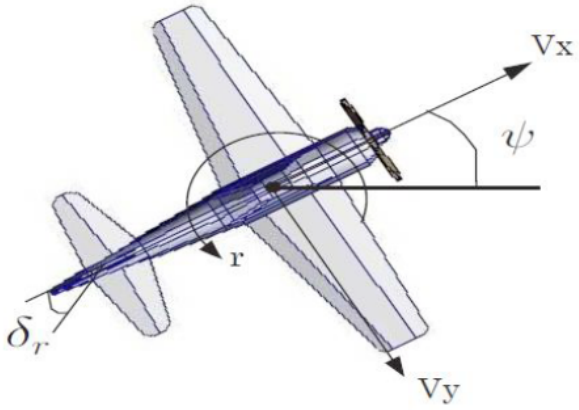

Figure 2: Yaw motion.

The desired trajectory design for the unmanned aerial vehicle is defined by the following equations:

$$\dot{x} = -r_d \sin(\xi)\dot{\xi} \tag{7}$$

$$\dot{y} = r_d \mathrm{Cos}(\xi)\dot{\xi} \tag{8}$$

where x, y are representing the position in the Cartesian plane where the fixed-wing UAV is located, r_d is the desired radius of the trajectory, and ψ is the yaw angle.

3. DESIGN OF THE CONTROL LAWS

It is worth mentioning that to control the height of the fixed-wing unmanned aerial vehicle, only a proportional derivative controller was applied, since for trajectory tracking the focus of the controllers is on the yaw angle and considering that for roll it is considered to be stable at zero degrees. To design the controller in altitude height, equations (2) - (4) are considered, this is because equation (1) represents the speed of the aircraft, but for the simulations of this work it is

considered as constant. Then, the altitude error is defined as $\tilde{e}_h = h_d - h$, with the h_d desired altitude and *h* is the actual or real altitude. The desired altitude is achieved by controlling the tilt angle, so we have defined an error for this angle, given by $\tilde{e}_\theta = \theta_d - \theta(t)$, and $\theta_d = \arctan(\tilde{e}_h / \varsigma)$ is the desired tilt angle, and ς denotes the length from the center of mass of the UAV to the nose of the UAV. Then, let us consider the equations (2)-(4), where the control input is defined. Thus, the proportional derivative (PD) [11] control is given by:

$$\delta_e = k_{ph}\tilde{e}_\theta + k_{dh}\dot{\tilde{e}}_\theta \tag{9}$$

where k_{ph} and k_{dh} are called position and velocity gains, respectively, of the control law for altitude. The proportional derivative control law for yaw angle is defined by [11]:

$$\delta_r = k_{p\psi}\tilde{e}_\psi + k_{d\psi}\dot{\tilde{e}}_\psi \tag{10}$$

with $k_{p\psi}$ and $k_{d\psi}$ are called position and velocity gains, from the control law for the yaw angle, respectively. To design the control law for yaw angle we need the equations (5)-(6), because with the yaw angle we can achieve or follow the desired trajectory. Thus, the yaw error is defined by $\tilde{e}_\psi = \psi_d - \psi$, $\psi_d = \xi + \pi/2$, ψ_d is the desired yaw angle and ψ represents the current angle of the UAV. The sliding mode-based controller is defined by [12]-[13]:

$$\delta_r = \frac{-N_r r - k_{1\psi}\dot{\tilde{e}}_\psi - \beta_x \operatorname{sgn}(s)}{N_{\delta r}} \tag{11}$$

where $k_{1\psi}$ and β_x are positive definite gains and the sliding surface is $s = r + k_{1\psi}\tilde{e}_\psi$. The control law based on nested saturations is given by [11]:

$$\delta_r = \frac{-N_r r - \sigma_2(k_{1\psi}z_2 + \sigma_1(k_{2\psi}z_1))}{N_{\delta r}} \tag{12}$$

with $k_{1\psi}$ and $k_{2\psi}$ are positive gains, $z_1 = \frac{a_1}{N_r}\psi + r$, $z_2 = r$, $a_1 > 0$. The membership functions used for the fuzzy controller are presented below. Figure **3** presents the membership functions corresponding to the position. Figure **4** shows the membership functions corresponding to the speed, and finally, Figure **5** shows the membership functions of the output. Table **1** presents the rules that were designed for the fuzzy logic-based controller, and the meaning of the acronyms in Table **1** are:

- LN: Long Negative.
- MN: Medium Negative.
- SN: Small Negative.
- Z: Zero.
- SP: Small Positive.
- MP: Medium Positive.
- LP: Long Positive

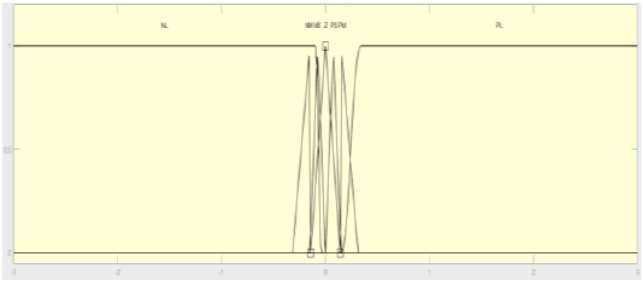

Figure 3: Membership functions for the position.

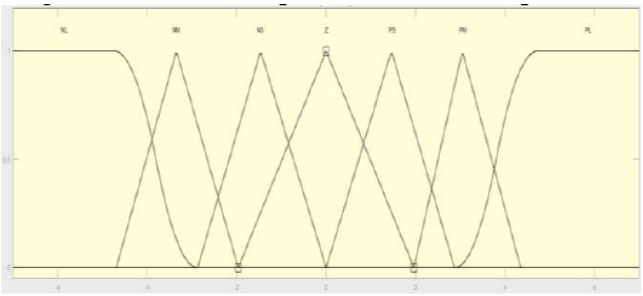

Figure 4: Membership functions for speed velocity.

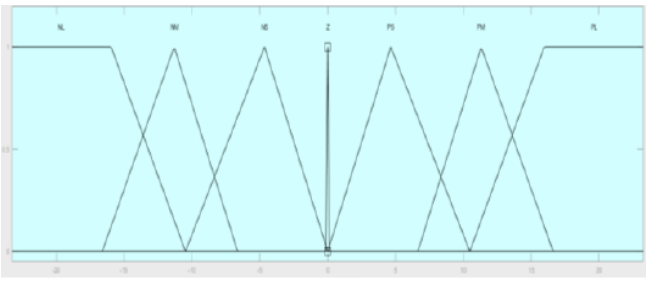

Figure 5: Membership functions for the output.

4. SIMULATION RESULTS

To describe the simulation results of the four controllers proposed for trajectory tracking, we have analyzed the results with the standard [13], see Table **2**, that is, the error signals and the control effort of each control law are analyzed.

$$l_2[e_h] = \sqrt{\frac{1}{T - t_0}\int_{t_0}^{T} \|e_h\|^2 \, dt} \tag{13}$$

$$l_2[\delta_e] = \sqrt{\frac{1}{T - t_0}\int_{t_0}^{T} \|\delta_e\|^2 \, dt} \tag{14}$$

Table 1: Rules for the Fuzzy Control

$e_p \downarrow, e_d \rightarrow$	LN	MN	SN	Z	SP	MP	LP
LN	LN	MN	MN	SN	Z	Z	Z
MN	LN	MN	MN	SN	Z	Z	MP
SN	LN	MN	MN	SN	Z	SP	MP
Z	MN	SN	SN	Z	SP	SP	MP
SP	MN	SN	Z	SP	MP	MP	LP
MP	MN	Z	Z	SP	MP	MP	LP
LP	Z	Z	Z	SP	MP	MP	LP

Table 2: L_2 -Norm for the Error and Control Effort

Controller	$l_2[e_\psi][grades]$	$l_2[\delta_r][grades]$
PD	0.5596	1.8067
Sliding modes	0.2999	19.3257
Nested saturation	3.2896	1.7166
Fuzzy logic	0.1567	2.4516

Figure **6** presents the altitude controller with the PD law.

Figure **7** presents the control law responses of the controllers, and based on Table **1** the controller that applied a minor control effort to achieve the desired trajectory is the methodology nested saturation, and the control law that applied a major control effort is the sliding mode control technique, and considering the chattering effect appreciated in the Figure **7**.

The control technique that presented a minor error is based on fuzzy logic (see Table **2**), and the major error is presented by the nested saturation methodology, see Table **2**. Figure **8** presents the error signal of each controller presented in this work. Figure **9** is presented the path following the fixed-wing UAV in the Cartesian plane, and Figure **10** is presented the response of the controllers in the x-y-z axes. In Figure **10**, it is appreciated that the objective of control is achieved by the controllers presented in this work.

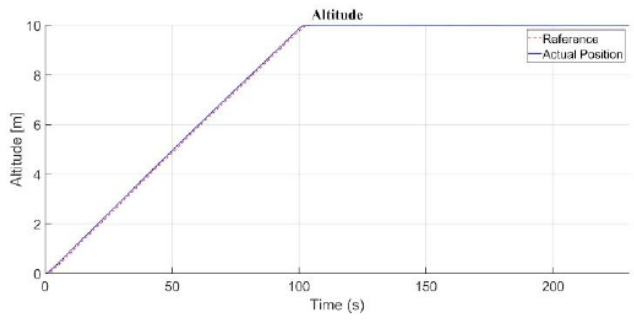

Figure 6: Altitude control with Proportional-Derivative controller.

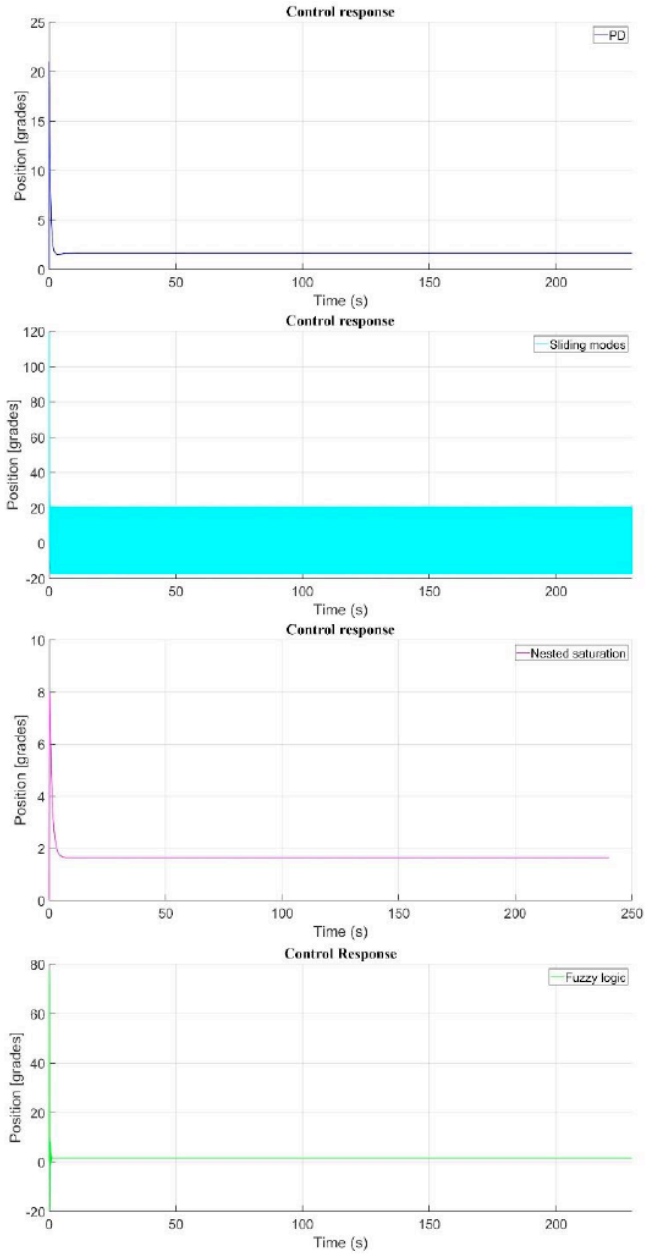

Figure 7: Control response of the yaw angle.

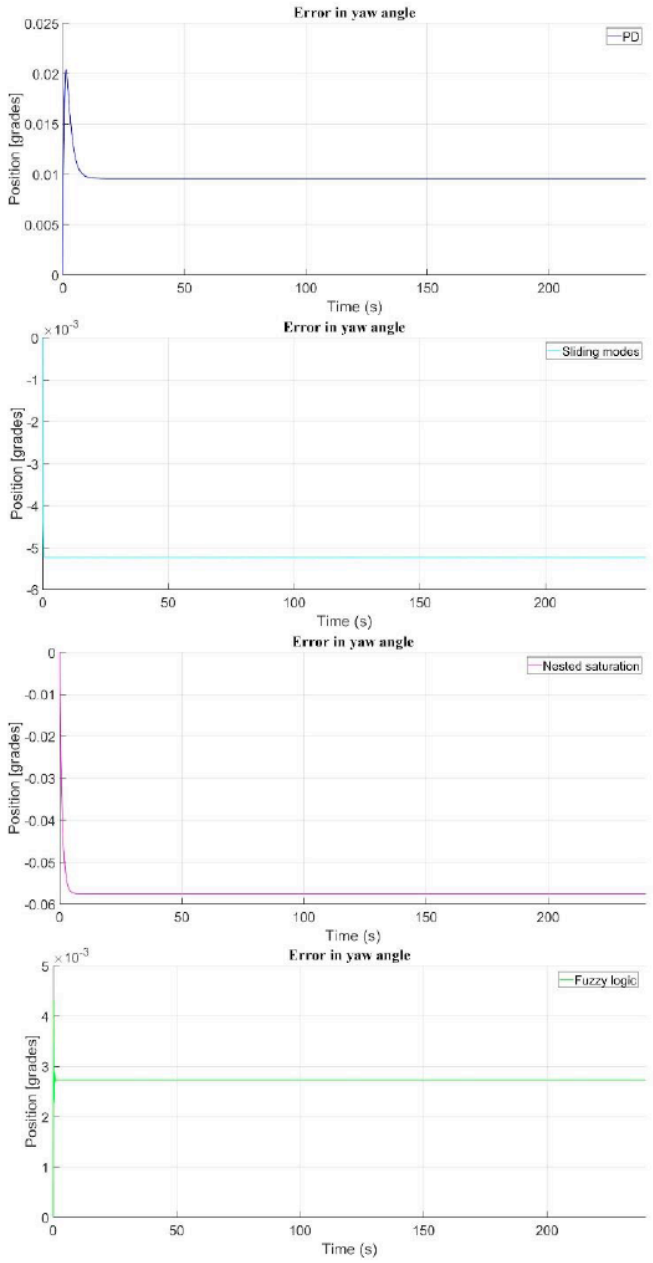

Figure 8: Error response in yaw angle.

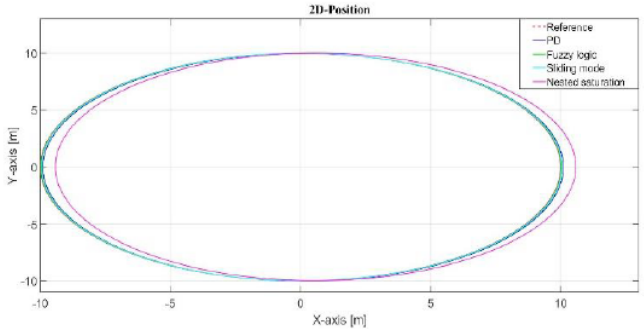

Figure 9: Position in the x-y axis (Path following).

5. CONCLUSIONS

This work has presented the comparison of four control laws applied to fixed-wing UAV with the objective of following a desired trajectory or path.

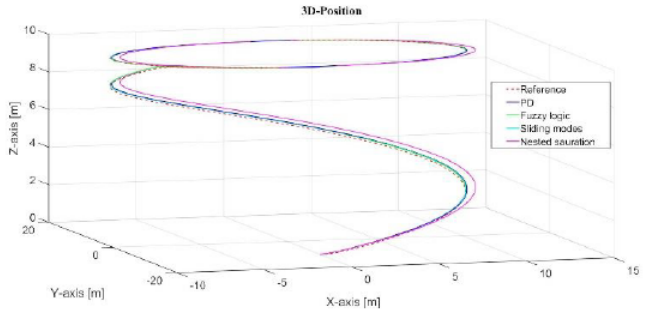

Figure 10: Position in the x-y-z axis (Path following).

And after several simulations and based on the analysis of the error and the effort of the controllers. The controller which presented a better response in control effort is based on nested saturation methodology, but the error response is bigger in comparison with the PD, sliding mode technique, and fuzzy logic.

The controller that presented a smaller error is the sliding modes technique, but it presented the chattering effect in the control signal and the control response is bigger in comparison with the PD, nested saturation, and fuzzy logic.

It should be mentioned that the four controllers achieved the desired trajectory.

FUNDING

This work was not financially supported by any grant.

CONFLICT OF INTEREST

The authors declare that a conflict of interest does not exist.

REFERENCES

[1] K. P. Valavanis, “Advances in Unmanned Aerial Vehicles”, Ed. Springer, ISBN: 1-4020-6113-4, 2007. https://doi.org/10.1007/978-1-4020-6114-1

[2] J. Guerrero and R. Lozano, “Flight Formation Control”, Ed. Wiley, ISBN: 184-82-1323-9, 2012. https://doi.org/10.1002/9781118387191

[3] E. Safwat, W. Zhang, A. Mohsen, and M. Kassem, “Design and Analysis of a Robust UAV Flight Guidance and Control System Based on a Modified Nonlinear Dynamic Inversion”, MDPI Applied Science, Vol. 9, Num. 17, pp. 1-25, 2019. https://doi.org/10.3390/app9173600

[4] I. Kaminer, A. Pascoal, E. Xargay, N. Hovakimyan, C. Cao, and V. Dobrokhodov, “Path Following for Unmanned Aerial Vehicles Using L1 Adaptive Augmentation of Commercial Autopilots”, Journal of Guidance, Control, and Dynamics, Vol. 33, No. 2, pp. 550-564, 2010. https://doi.org/10.2514/1.42056

[5] H. Zhou, H. Xiong, Y. Liu, N. Tan, and L. Chen, “Trajectory Planning Algorithm of UAV Based on System Positioning Accuracy Constraints”, Vol. 9, No. 2, pp. 1-21, 2020. https://doi.org/10.3390/electronics9020250

[6] L. Sun and R. W. Beard, “Trajectory Tracking for Unmanned Aerial Vehicles with Autopilot in the Loop”, Journal in Computer Science, pp. 1-6, 2012.

[7] G. Tang, Z. Hou, C. Claramunt, and X. Hu, “UAV Trajectory Planning in a Port Environment ”, Vol. 8, No. 8, pp. 1-12, 2020. https://doi.org/10.3390/jmse8080592

[8] M. V. Cook, “Flight Dynamics Principles”, Second edition, Ed. Elsevier, ISBN: 978-0-7506-6927-6, 2007.

[9] D. Mclean, “Automatic Flight Control Systems”, Ed. Prentice hall International, ISBN: 0-13-054008-0, 1990.

[10] Brian L. Stevens and Frank L. Lewis, “Advances in Unmanned Aerial Vehicles”, Ed. John Wiley and Sons, ISBN: 0-471-61397-5, 1992.

[11] T. Espinoza-Fraire, A. Dzul. R. Parada, and A. Sáenz, “Design of Control Laws and State Observers for Fixed-wing UAVs: Simulation and Experimental Approaches”, Ed. Elsevier, 978-0-323-95405-1.

[12] J.J. Slotine and W. Li, “Applied Nonlinear Control”, Prentice Hall, ISBN: 0-1304-0890-5 USA, 1991.

[13] H. K. Khalil, “Nonlinear Systems”, Ed. Prentice Hall, ISBN: 0-13-067389-7, 1996.

Received on 20-10-2024 Accepted on 28-11-2024 Published on 10-12-2024

https://doi.org/10.31875/2409-9694.2024.11.10